A nanodiamond-tapered fiber system with high single-mode coupling efficiency

Tim Schröder,[1,*] Masazumi Fujiwara,[2,3] Tetsuya Noda,[2,3] Hong-Quan Zhao,[2,3] Oliver Benson,[1] and Shigeki Takeuchi[2,3,4]

[1]*Institute of Physics, AG Nano-Optik, Humboldt-Universitt zu Berlin, Newtonstr. 15, 12489 Berlin, Germany*
[2]*Research Institute for Electronic Science, Hokkaido University, Sapporo, Hokkaido 001-0021, Japan*
[3]*The Institute of Scientific and Industrial Research, Osaka University, Ibaraki, Osaka 567-0047, Japan*
[4]*takeuchi@es.hokudai.ac.jp*

[*]*tim.schroeder@physik.hu-berlin.de*

Abstract: We present a fiber-coupled diamond-based single photon system. Single nanodiamonds containing nitrogen vacancy defect centers are deposited on a tapered fiber of 273 nanometer in diameter providing a record-high number of 689,000 single photons per second from a defect center in a single-mode fiber. The system can be cooled to cryogenic temperatures and coupled evanescently to other nanophotonic structures, such as microresonators. The system is suitable for integrated quantum transmission experiments, two-photon interference, quantum-random-number generation and nano-magnetometry.

© 2012 Optical Society of America

OCIS codes: (270.5585) Quantum information and processing; (060.1155) All-optical networks; (230.6080) Sources; (130.3120) Integrated optics devices.

References and links

1. J. L. O'Brien, "Optical quantum computing," Science **318**, 1567–1570 (2007).
2. J. L. O'Brien, A. Furusawa, and J. Vuckovic, "Photonic quantum technologies," Nature Photon. **3**, 687–95 (2009).
3. D. Stick, W. K. Hensinger, S. Olmschenk, M. J. Madsen, K. Schwab, and C. Monroe, "Ion trap in a semiconductor chip," Nature Phys. **2**, 36–39 (2006).
4. E. Vetsch, D. Reitz, G. Sagué, R. Schmidt, S. T. Dawkins, and A. Rauschenbeutel, "Optical interface created by laser-cooled atoms trapped in the evanescent field surrounding an optical nanofiber," Phys. Rev. Lett. **104**, 203603 (2010).
5. A. Blais, J. Gambetta, A. Wallraff, D. I. Schuster, S. M. Girvin, M. H. Devoret, and R. J. Schoelkopf, "Quantum-information processing with circuit quantum electrodynamics," Phys. Rev. A **75**, 032329 (2007).
6. P. Zoller T. Beth, D. Binosi, R. Blatt, H. Briegel, D. Bruss, T. Calarco, J. I. Cirac, D. Deutsch, J. Eisert, A. Ekert, C. Fabre, N. Gisin, P. Grangiere, M. Grassl, S. Haroche, A. Imamoglu, A. Karlson, J. Kempe, L. Kouwenhoven, S. Krall, G. Leuchs, M. Lewenstein, D. Loss, N. Latkenhaus, S. Massar, J. E. Mooij, M. B. Plenio, E. Polzik, S. Popescu, G. Rempe, A. Sergienko, D. Suter, J. Twamley, G. Wendin, R. Werner, A. Winter, J. Wrachtrup, and A. Zeilinger, "Quantum information processing and communication," Eur. Phys. J. D **36**, 203–228 (2005).
7. M. Wallquist, K. Hammerer, P. Rabl, M. Lukin, and P. Zoller, "Hybrid quantum devices and quantum engineering," Phys. Scr. **2009**, 014001 (2009).
8. F. Jelezko and J. Wrachtrup, "Single defect centres in diamond: A review," Phys. Status Solidi A **203**, 3207–3225 (2006).
9. I. Aharonovich, A. D. Greentree, and S. Prawer, "Diamond photonics," Nature Photon. **5**, 397–405 (2011).
10. P. Siyushev, F. Kaiser, V. Jacques, I. Gerhardt, S. Bischof, H. Fedder, J. Dodson, M. Markham, D. Twitchen, F. Jelezko, and J. Wrachtrup, "Monolithic diamond optics for single photon detection," Appl. Phys. Lett. **97**, 241902 (2010).

#162699 - $15.00 USD Received 8 Feb 2012; revised 23 Mar 2012; accepted 26 Mar 2012; published 23 Apr 2012

11. T. Schröder, F. Gädeke, M. J. Banholzer, and O. Benson, "Ultrabright and efficient single-photon generation based on nitrogen-vacancy centres in nanodiamonds on a solid immersion lens," New J. Phys. **13**, 055017 (2011).
12. L. Marseglia, J. P. Hadden, A. C. Stanley-Clarke, J. P. Harrison, B. Patton, Y.-L. D. Ho, B. Naydenov, F. Jelezko, J. Meijer, P. R. Dolan, J. M. Smith, J. G. Rarity, and J. L. O'Brien, "Nanofabricated solid immersion lenses registered to single emitters in diamond," Appl. Phys. Lett. **98**, 133107 (2011).
13. G. Balasubramanian, P. Neumann, D. Twitchen, M. Markham, R. Kolesov, N. Mizuochi, J. Isoya, J. Achard, J. Beck, J. Tissler, V. Jacques, P. R. Hemmer, F. Jelezko, and J. Wrachtrup, "Ultralong spin coherence time in isotopically engineered diamond," Nat. Mater. **8**, 383–387 (2009).
14. G. de Lange, Z. H. Wang, D. Riste, V. V. Dobrovitski, and R. Hanson, "Universal dynamical decoupling of a single solid-state spin from a spin bath," Science **330**, 60–63 (2010).
15. S. Pezzagna, B. Naydenov, F. Jelezko, J. Wrachtrup, and J. Meijer, "Creation efficiency of nitrogen-vacancy centres in diamond," New J. Phys. **12**, 065017 (2010).
16. T. M. Babinec, H. J. M., M. Khan, Y. Zhang, J. R. Maze, P. R. Hemmer, and M. Loncar, "A diamond nanowire single-photon source," Nat. Nanotechnol. **5**, 195–199 (2010).
17. A. Faraon, P. E. Barclay, C. Santori, K.-M. C. Fu, and R. G. Beausoleil, "Resonant enhancement of the zero-phonon emission from a colour centre in a diamond cavity," Nature Photon. **5**, 301–305 (2011).
18. T. Schröder, A. W. Schell, G. Kewes, T. Aichele, and O. Benson, "Fiber-integrated diamond-based single photon source," Nano Lett. **11**, 198–202 (2011).
19. F. Jelezko, T. Gaebel, I. Popa, M. Domhan, A. Gruber, and J. Wrachtrup, "Observation of coherent oscillation of a single nuclear spin and realization of a two-qubit conditional quantum gate," Phys. Rev. Lett. **93**, 130501 (2004).
20. D. E. Chang, A. S. Sorensen, E. A. Demler, and M. D. Lukin, "A single-photon transistor using nanoscale surface plasmons," Nat. Phys. **3**, 807–812 (2007).
21. K. Y. Han, K. I. Willig, E. Rittweger, F. Jelezko, C. Eggeling, and S. W. Hell, "Three-dimensional stimulated emission depletion microscopy of nitrogen-vacancy centers in diamond using continuous-wave light," Nano Lett. **9**, 3323–3329 (2009).
22. P. C. Maurer, J. R. Maze, P. L. Stanwix, L. Jiang, A. V. Gorshkov, A. A. Zibrov, B. Harke, J. S. Hodges, A. S. Zibrov, A. Yacoby, D. Twitchen, S. W. Hell, R. L. Walsworth, and M. D. Lukin, "Far-field optical imaging and manipulation of individual spins with nanoscale resolution," Nat. Phys. **6**, 912–918 (2010).
23. G. Balasubramanian, I. Y. Chan, R. Kolesov, M. Al-Hmoud, J. Tisler, C. Shin, C. Kim, A. Wojcik, P. R. Hemmer, A. Krueger, T. Hanke, A. Leitenstorfer, R. Bratschitsch, F. Jelezko, and J. Wrachtrup, "Nanoscale imaging magnetometry with diamond spins under ambient conditions," Nature **455**, 648–651 (2008).
24. J. R. Maze, P. L. Stanwix, J. S. Hodges, S. Hong, J. M. Taylor, P. Cappellaro, L. Jiang, M. V. G. Dutt, E. Togan, A. S. Zibrov, A. Yacoby, R. L. Walsworth, and M. D. Lukin, "Nanoscale magnetic sensing with an individual electronic spin in diamond," Nature **455**, 644–647 (2008).
25. F. Le Kien, S. Dutta Gupta, V. I. Balykin, and K. Hakuta, "Spontaneous emission of a cesium atom near a nanofiber: efficient coupling of light to guided modes," Phys. Rev. A **72**, 032509 (2005).
26. M. Fujiwara, K. Toubaru, T. Noda, H.-Q. Zhao, and S. Takeuchi, "Highly efficient coupling of photons from nanoemitters into single-mode optical fibers," Nano Lett. **11**, 4362–4365 (2011).
27. R. Hanbuy Brown and R. Q. Twiss, "Correlation between photons in two coherent beams of light," Nature **177**, 27–29 (1956).
28. S.-J. Yu, M.-W. Kang, H.-C. Chang, K.-M. Chen, and Y.-C. Yu,

    Bright fluorescent nanodiamonds: no photobleaching and low cytotoxicity, J. Am. Chem. Soc. **127**, 17604–17605 (2005).
29. B. R. Smith, D. W. Ingliss, B. Sandness, J. R. Rabeau, A. V. Zvyagin, D. Gruber, C. J. Noble, R. Vogel, E. Osawa, and T. Plakhotnik,

    Five-nanometer diamond with luminescent nitrogen-vacancy defect centers, Small **5**, 1649–1653 (2009).
30. M. Fujiwara, K. Toubaru, and S. Takeuchi, "Optical transmittance degradation in tapered fibers," Opt. Express **19**, 8596–8601 (2011).
31. A. Stefanov, N. Gisin, O. Guinnard, L. Guinnard, and H. Zbinden, "Optical quantum random number generator," J. Mod. Opt. **47**, 595–598 (2000).
32. M. Wahl, M. Leifgen, M. Berlin, T. Rohlicke, H.-J. Rahn, and O. Benson, "An ultrafast quantum random number generator with provably bounded output bias based on photon arrival time measurements," Appl. Phys. Lett. **98**, 171105 (2011).
33. C. K. Hong, Z. Y. Ou, and L. Mandel, "Measurement of subpicosecond time intervals between two photons by interference," Phys. Rev. Lett. **59**, 2044–2046 (1987).
34. H. Bernien, L. Childress, L. Robledo, M. Markham, D. Twitchen, and R. Hanson, "Two-photon quantum interference from separate nitrogen vacancy centers in diamond," Phys. Rev. Lett. **108**, 043604 (2012).
35. Y. Shen, T.M. Sweeney, and H. Wang, "Zero-phonon linewidth of single nitrogen vacancy centers in diamond nanocrystals," Phys. Rev. B **77**, 033201 (2008).
36. R. B. Patel, A. J. Bennett, I. Farrer, C. A. Nicoll, D. A. Ritchie, and A. J. Shields, "Two-photon interference of the emission from electrically tunable remote quantum dots," Nature Photon. **4**, 632–635 (2010).

#162699 - $15.00 USD Received 8 Feb 2012; revised 23 Mar 2012; accepted 26 Mar 2012; published 23 Apr 2012
(C) 2012 OSA

37. M. Gregor, R. Henze, T. Schröder, and O. Benson, "On-demand positioning of a preselected quantum emitter on a fiber-coupled toroidal microresonator," Appl. Phys. Lett. **95**, 153110 (2009).
38. J. Wolters, A. W. Schell, G. Kewes, N. Nüsse, M. Schoengen, H. Doscher, T. Hannappel, B. Lochel, M. Barth, and O. Benson, "Enhancement of the zero phonon line emission from a single nitrogen vacancy center in a nanodiamond via coupling to a photonic crystal cavity," Appl. Phys. Lett. **97**, 141108 (2010).
39. A. Faraon, I. Fushman, D. Englund, N. Stoltz, P. Petroff, and J. Vuckovic, "Coherent generation of nonclassical light on a chip via photon-induced tunneling and blockade," Nature Phys. **4**, 859–863 (2008).
40. J. Hwang, M. Pototschnig, R. Lettow, G. Zumofen, A. Renn, S. Gotzinger, and V. Sandoghdar, "A single-molecule optical transistor," Nature **460**, 76–80 (2009).
41. H. F. Hofmann, K. Kojima, S. Takeuchi, and K. Sasaki, "Optimized phase switching using a single-atom nonlinearity," J Optics B **5**, 218–221 (2003).
42. K. Kojima, H. F. Hofmann, S. Takeuchi, and K. Sasaki, "Efficiencies for the single-mode operation of a quantum optical nonlinear shift gate," Phys. Rev. A **70**, 013810 (2004).

In recent years there has been an increasing effort to implement scalable integrated quantum technologies [1, 2]. Besides miniaturized or fiber-coupled atom or ion traps [3, 4], promising approaches rely on solid-state systems [5–7]. Single defect centers in diamond have been recognized as ideal building blocks for an integrated platform [8, 9]. They provide optical stability, even at room temperature, high emission rate of single photons [10–12], and a long electron spin coherence time [13, 14]. Their capability of integration into photonic or plasmonic nanostrutures has been demonstrated in principle [15–18]. However, for basic quantum optical elements such as quantum logic gates [19] or single photon transistors [20], there exist challenging benchmarks. Photons have to be generated with highest possible emission rate, they have to be coupled efficiently to single-mode waveguides or fibers, and complex routing to connect various elements should be possible. Beyond quantum applications a robust integration and controlled optical access will introduce single defect centers as classical ultra-low intensity optical switches or as local probes for microscopy [21,22] and magnetometry [23,24] on the nanoscale.

In this letter we report an ultra-bright fiber-coupled diamond based single photon source where $689 \pm 12\,kcps$ of single photons are coupled directly to a single-mode fiber. In our experiment an integrated nanodiamond - tapered-fiber - system is presented, consisting of ultra-thin single-mode tapered fibers with a diameter of down to 273 nm that were equipped with nanodiamonds smaller than 150 nm containing nitrogen vacancy centers (NVs). It has been theoretically predicted that single photons from atoms can be coupled to a tapered single-mode optical fiber very efficiently when the diameter of the tapered fiber becomes a half of the wavelength of the emitted photons [25]. Recently, we reported coupling of fluorescence light from a colloidal quantum dot to a tapered fiber [26]. However, these dots suffer from significant blinking and bleaching, and are not suitable as stable single photon sources or sensors. The presented system uses for the first time a solid-state quantum emitter (single NV defect center) which is free from these difficulties.

Tapered fibers were fabricated from standard single-mode optical fibers (Thorlabs, 630HP) by a procedure described elsewhere [26]. The emission of either single or multiple NVs was efficiently collected via the fiber mode and guided to the two ends of the fiber as schematically shown in Fig. 1(a).

For the preparation of the single photon system, a dip-coating technique was developed that allows for the controlled deposition of nanodiamonds. A small droplet of a suitable dense aqueous nanodiamond solution was given onto the facet of a thin glass rod with a diameter of about 1 mm, see Fig. 1(b). While measuring the transmission of a 640 nm laser through the fiber the tapered fiber region was dipped into the solution. By moving the tapered fiber via a linear stage along the fiber axis through the droplet, nanodiamonds were deposited. During deposition procedure the light scattered off deposited particles was monitored. In this way it was possible to estimate the number of deposited particles as can be seen in Fig. 2(a). By in-situ measuring the transmission of the fiber, overall scattering losses were evaluated. For example, controlled

#162699 - $15.00 USD Received 8 Feb 2012; revised 23 Mar 2012; accepted 26 Mar 2012; published 23 Apr 2012
(C) 2012 OSA

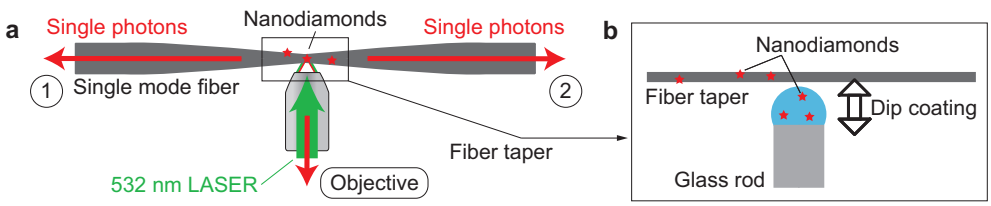

Fig. 1. (a) Schematic of a tapered fiber equipped with nanodiamonds, excited with a 532 nm laser, single photons were collected either through the objective or the fiber ends. Tapered fibers with diameters down to 273 nm were applied. 1 and 2 indicate fiber end one and fiber end two, respectively. (b) Schematic of dip coating technique: A small droplet of an aqueous nanodiamond solution was given onto the facet of a thin glass rod with a diameter of about 1 mm. The tapered fiber was dipped into the solution. By moving the tapered fiber via a linear stage along the fiber axis through the droplet, nanodiamonds were deposited. This deposition was controlled by the laser scattering signal of the deposited nanoparticles and allowed for controlling the deposition of an approximate number of scatterers.

depostion of 16 scatterers on a tapered fiber with a diameter of about 360 nm was performed, while its transmission loss was only 4 %, a typical value for all examined tapered fibers.

To find and analyse deposited nanoparticles a microscope image of the tapered fiber was taken. To make the particles optically visible red laser light was send through the fiber. At the position of nanoparticles, parts of the guided light is scatterd and collected by the objective ($NA = 0.8$) of the microscope. Such an image, taken with a conventional CCD camera, is depicted in Fig. 2(a), four scatterers can be seen. To identify single photon emitting defect centers, lateral x-y-intensity scans with a home-built confocal microscope featuring a multi-mode fiber as pinhole (Thorlabs, 1550HP, core diameter $\sim 10\,\mu m$) and a x-y-piezo scanner were performed, see Fig. 2(a). For excitation, a CW 532 nm laser was used, while the laser fluorescence was blocked with two 565 nm long pass filters. Doing so, fluorescent particles as the NV were identified. Such a scan is shown at the bottom panel of Fig. 2(a) where a single nanodiamond containing multiple NVs is present. Both panels (top and bottom) in Fig. 2(a) depict the same tapered fiber region. By comparing both images, fluorescent nanoparticles can be distinguished from merely scattering ones.

First evidence for the fluorescence stemming indeed from NV centers can be retrieved from spectral analysis. The black and the red graph in Fig. 2(b) show the fluorescence of the nanodiamond coupled to the fiber from Fig. 2(a) collected by the confocal microscope and by one end of the fiber, respectively, when excited with $500\,\mu W$. The spectrum collected by the fiber appears red-shifted due to fiber background fluorescence and due to wavelength dependent transmission of the laser light filter stage. This free space filter stage with two aspherical lenses for fiber in- and out-coupling shows high chromatic abberation. Therefore wavelengths around 800 nm have a higher transmission than wavelengths around 600 nm. Nevertheless ZPLs of the neutral and of the negatively charged NV can be identified in both spectra around 575 nm and 637 nm, originating from several NVs. Fig. 2(c) shows a fluorescence spectrum of a single NV excited with $500\,\mu W$. The peaks in the spectra around 575 nm indicate a neutral NV. The spectrum shows the emission collected by the confocal microscope and by one end of the fiber, displayed with black and red graphs, respectively. The intensity of these peaks was used to normalize both spectra. The spectrum collected by the fiber was corrected by substraction of the fiber fluorescence background.

A Hanbury Brown and Twiss setup was used to perform auto- and cross-correlation measurements [27]. Photon statistics can be derived from the normalized second-order autocorrelation

#162699 - $15.00 USD Received 8 Feb 2012; revised 23 Mar 2012; accepted 26 Mar 2012; published 23 Apr 2012
(C) 2012 OSA

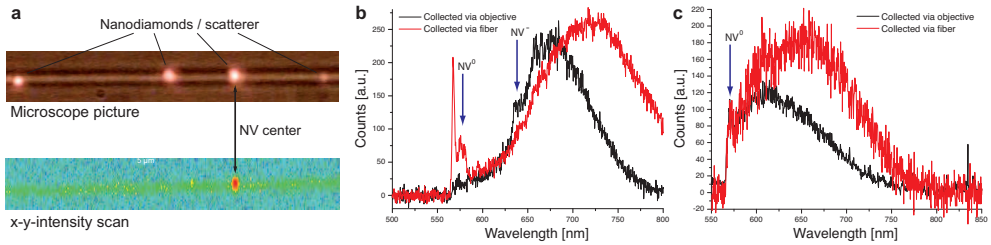

Fig. 2. (a) Top: Microscope picture of a 40 μm long tapered fiber section. Laser is guided through the fiber. The scattered light from four scatterers is visible. Bottom: x-y-intensity scan of the same region. While the tapered fiber is scanned, 532 nm laser light is focused on the tapered fiber. The laser is blocked with a 565 nm long pass filter before the detection of fluorescence $>$ 565 nm. One of the four scatterers contains several nitrogen vacancy centers. (b) Spectrum of the fluorescence of the light emitter depicted in the lower panel of Fig. 2(a) at excitation intensity of 500 μW. Several nitrogen vacancy centers contribute to the emission. Clearly visible are the zero phonon lines of the neutral (575 nm) and the negatively charged (637 nm) centers. (c) Spectrum of the fluorescence of a single neutral nitrogen vacancy center excited with 500 μW, normalized to the zero phonon line at 575 nm. The black and red line in (b) and (c) represent the fluorescence collected via an air objective and via one end of the fiber, respectively. The red spectra appear redshifted due to chromatic dependence of the fiber filter stage transmission.

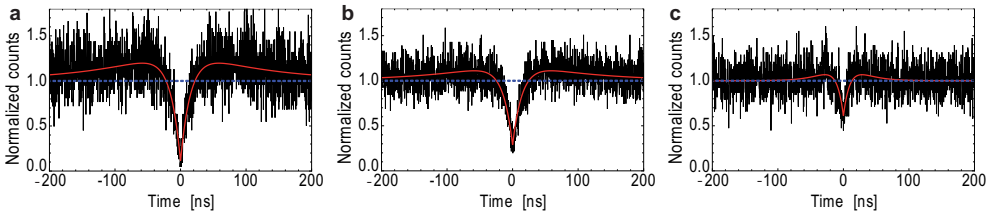

Fig. 3. (a) Normalized auto-correlation function of the same single NV center as in Fig. 2(c). Light was collected via the air objective (see Fig. 1(a)). A deep anti-bunching dip $g^{(2)}(0) = 0.11$ is visible. According to the spectrum in Fig. 2(c) this correlation measurement confirms a single neutral NV defect center as single photon source. (b) Cross-correlation measurement for fiber end one with the photons collected via the objective (see Fig. 1(a)). $g^{(2)}(0) = 0.29$ proves single photon statistics for the fiber coupled light. For an equivalent measuremtent for fiber end two $g^{(2)}(0)$ was 0.29 (not displayed for redundance). (c) Cross-correlation measurements between the two fiber ends. The anti-bunching dip $g^{(2)}(0) = 0.61$ is slightly higher than 0.5, yet indicating strong quantum character of the light. The correlation functions in (a), (b), (c) were taken at excitation intensities of 450 μW, 500 μW and 400 μW, respectively.

#162699 - $15.00 USD Received 8 Feb 2012; revised 23 Mar 2012; accepted 26 Mar 2012; published 23 Apr 2012
(C) 2012 OSA

function

$$g^{(2)}(\tau) = \frac{\langle I(t)\, I(t+\tau)\rangle}{\langle I(t)\rangle^2}.$$

In Fig. 3(a) the auto-correlation function of the same NV as depicted in Fig. 2(c) is displayed. The data in Fig. 3(a) was collected via the confocal microscope. A deep anti-bunching dip $g^{(2)}(0) = 0.11 < 0.5$ is visible. This proves, that the collected light originates from a single photon emitter, in this case from a single neutral NV, in reference to the spectrum in Fig. 2(c). For both fiber ends cross-correlation measurements with the photons collected via the objective were performed (see Fig. 3(b)). $g^{(2)}(0) = 0.29$ and $g^{(2)}(0) = 0.29$ for fiber end one and fiber end two (not shown here, see Fig. 1(a)), respectively. This clearly proves that the photon flux in the fiber is from a single light emitter even in the cross correlation measurement. The less pronounced dip indicates higher background fluorescence generated mainly in the tapered fiber region. This background has stronger influence on the cross-correlation measurements taken between the two fiber ends as it is present in both channels of the HBT setup Fig. 3(c). Therefore the anti-bunching dip $g^{(2)}(0) = 0.61$ is slightly higher than 0.5, yet indicating strong quantum character of the light. All correlation measurements were performed while blocking the laser light with a 565 nm long-pass filter.

To estimate the total amount of single photons coupled from the NV emission into the single-mode fiber, saturation measurements and setup efficiency analysis were carried. For saturation measurements, detected photon events were recorded at different excitation intensities. Fitting to the experimental curves was done according to $R(I) = \frac{R_{\mathrm{Inf}}\, I}{I_{\mathrm{Sat}}+I} + (\alpha)I + \beta$, where R is the single photon count rate, R_{Inf} the count rate at infinite excitation intensities, I the excitation intensity, I_{Sat} the saturation excitation intensity, while α and β are fit parameters for linear background stemming from the diamond and tapered fiber and additional background such as dark counts from the avalanche photo diodes (APD) and residual stray light, respectively.

For the same neutral NV as in Fig. 2(c), this analysis reveals $74 \pm 2\,kcps$, $104 \pm 1\,kcps$ and $107 \pm 3\,kcps$ for collection via the objective, fiber end one and fiber end two, respectively (see Fig. 1(a) and Fig. 4). In total $211 \pm 3\,kcps$ single-mode single photons originating from the fiber were measured. The efficiencies to detect such a fiber coupled single photon was limited by the transmission of the filter stages and the quantum efficiency of the APDs (taken from APD datasheets). These efficiencies were determined to $\nu = 0.33$ for emission from fiber end one and $\nu = 0.29$ for fiber end two (see Fig. 1(a)). Taking these efficiencies into consideration, a total number of $(689 \pm 12) \cdot 10^3$ single photons are coupled to the single-mode fiber at saturation intensities. This is to our knowledge the highest reported number of single-mode fiber coupled single photons originating from an NV in diamond. This number corresponds to an estimated nearfield coupling efficiency of 1.7 %, assuming an internal NV quantum efficiency of one [28] and using a lifetime of 25 ns [29] for a nanodiamond ($690000 \cdot 25\,\mathrm{ns} = 1.7\,\%$). We would like to point out that sending all collected photons to one end of the fiber is straightforward, e.g., by adding a fiber Bragg grating mirror to the other side [26].

Despite the presented advantages, some drawbacks of the tapered fiber system have to be pointed out. The tapered fiber is very sensitive to any kind of particle deposition for example caused by dust from normal air environments where its transmission degrades within minutes. Therefore the tapered fiber has to be operated in a clean-room environment of at least class 1000 [30]. If operated in a class 10 environment, transmission endures for months as was tested within our clean-room facilities. Background fluorescence plays a major role when working in the regime of single photons. Another possible difficulty may be the fiber background fluorescence originating from fiber coupled excitation laser light could not always be neglected. At 1 mW excitation, a typical NV excitation power for our setup, 10 nW are coupled to the fiber and cause background in the orders of magnitude of 10^3 to 10^4 kcps. To overcome this

#162699 - $15.00 USD Received 8 Feb 2012; revised 23 Mar 2012; accepted 26 Mar 2012; published 23 Apr 2012
(C) 2012 OSA

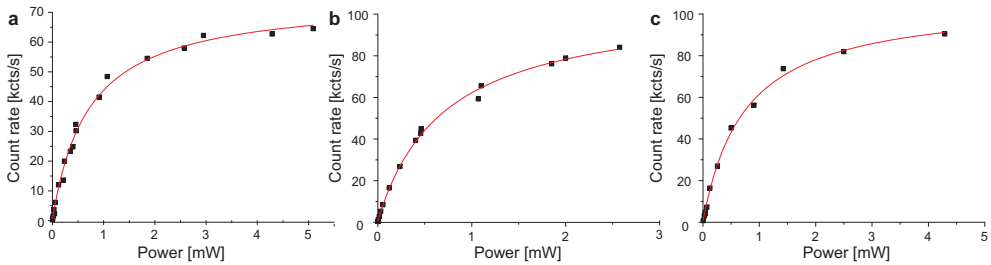

Fig. 4. (a,b,c) Saturation measurements of the NV from Fig. 2(c). Fitting (red solid lines) was done according to text. This analysis reveals (a) 74 ± 2 kcps, (b) 104 ± 1 kcps and (c) 107 ± 3 kcps for collection via the objective, fiber end one and fiber end two, respectively (see Fig. 1(a)). In total 211 ± 3 kcps single-mode single photons from the fiber were measured. The efficiencies to measure a single photon from the tapered region are $\nu = 0.33$ for emission from fiber end one and $\nu = 0.29$ for fiber end two. Taking these efficiencies into consideration, a total number of $(689 \pm 12) \cdot 10^3$ single photons are coupled to the single-mode fiber at saturation intensities.

problem, we have found that reduction of the fluorescence can be achieved with a bleaching method. About $100\,\mu W$ 532 nm laser light was guided for several minuntes up to several ten minutes through the fiber to the tapered region. By doing so, background was reduced one or two orders of magnitude. Over a time period of ten minutes, part of the fluorescence recovered. When we adopted this bleaching method, we were able to obtain $g^{(2)}(0) = 0.28$ for an NV center, taken several ten minutes after bleaching. Note also, that the coupling efficiency of the laser pump to the tapered fiber mode can be controlled by the laser polarization. By changing the excitation laser light from circular to linear polarization and by appropriate rotation, background could be reduced by a factor of up to six.

The correlation measurement shown in Fig. 3(c) already demonstrates that the tapered fiber represents a beam splitter. In order to quantify the branching ratio we quantitatively evaluated fluorescence spectra taken from a single nanodiamond at both fiber ends, see Fig. 5. We found a splitting ratio of 56:44. Such an integrated nearly 50:50 beamsplitter can be exploited for the realization of a quantum number generator [31, 32] or for generation of indistinguishable photons for a Hong-Ou-Mandel interference experiment [33]. Such an experiment with NVs has been shown for bulk diamond [34], but not yet for nanocrystals as it is more challenging to find lifetime limited emitters with slow spectral diffusion [35]. For the latter experiment a pulsed excitation with the tapered fiber at low temperatures (appr. 4 K) and a length difference of the two fiber ends matching the time difference between repeated excitation events can be used [36]. Indeed, we have successfully cooled a tapered fiber with a diameter of 300 nm to 7 K using our home-built cryostat system (results not shown) [30].

Moreover, the NV center - tapered fiber system can be mounted on a piezo translation stage and used as a nanoprobe [37]. In this way the NV center on the tapered fiber can be coupled evanescently to microresonators in order to enhance the spontaneous emission rate [37,38] or to locally probe the magnetic field via the NV center's electron spin [23]. Finally, the tapered fiber system as opposed to other fiber-coupling architectures, e. g. end-facet coupling [18], allows for measurements in transmission. This is a requirement for the implementation of single photon nonlinearities [39], single photon transistors [40] or quantum phase gates [41, 42].

In summary, a new diamond based single photon system was presented. Up to 689,000 single photons from a nitrogen vacancy defect center in nanodiamonds are coupled to a single-mode fiber at saturation intensities. With the additional ability of cryogenic operation and evanescent

#162699 - $15.00 USD Received 8 Feb 2012; revised 23 Mar 2012; accepted 26 Mar 2012; published 23 Apr 2012
(C) 2012 OSA

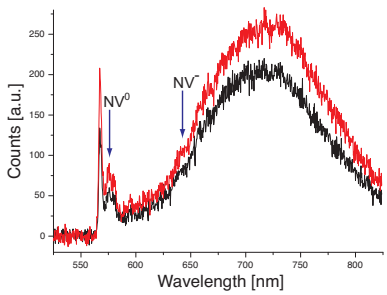

Fig. 5. (a) Spectra of several NVs from a single nanodiamond measured via fiber end one and fiber end two (see Fig. 1(a)), depicted with a black and a red line, respectively. The integrated intensities have a ratio of 56:44. Blue arrows indicate the zero phonon lines of neutral (575 nm) and negatively charged (637 nm) centers.

coupling to other nanophotonic structures our system represents a flexible tool for integrated quantum technology and nanophotonics.

Acknowledgment

TS and OB acknowledge financial support of the BMBF (KEPHOSI) and DFG Forschergruppe FOR1493. MF, TN, H-QZ, and ST acknowledge financial support from MIC-SCOPE, JST-CREST, MEXT-KAKENHI Quantum Cybernetics (No. 21102007), JSPS-KAKENHI (Nos. 20244062, 21840003, 23244079, and 23740228), JSPS-FIRST, Project for Developing Innovation Systems of MEXT, G-COE program, and Research Foundation for Opto-Science and Technology. The authors thank Prof. Jörg Wrachtrup, Dr. Helmut Fedder, both University Stuttgart, and Prof. Fedor Jelesko, University of Ulm, for providing the nanodiamond solution.